## PALEONTOLOGY

# Eggshell geochemistry reveals ancestral metabolic thermoregulation in Dinosauria

Robin R. Dawson[1]\*, Daniel J. Field[2,1], Pincelli M. Hull[1], Darla K. Zelenitsky[3], François Therrien[4], Hagit P. Affek[5,1]

Studying the origin of avian thermoregulation is complicated by a lack of reliable methods for measuring body temperatures in extinct dinosaurs. Evidence from bone histology and stable isotopes often relies on uncertain assumptions about the relationship between growth rate and body temperature, or the isotopic composition ($\delta^{18}O$) of body water. Clumped isotope ($\Delta_{47}$) paleothermometry, based on binding of $^{13}C$ to $^{18}O$, provides a more robust tool, but has yet to be applied across a broad phylogenetic range of dinosaurs while accounting for paleoenvironmental conditions. Applying this method to well-preserved fossil eggshells demonstrates that the three major clades of dinosaurs, Ornithischia, Sauropodomorpha, and Theropoda, were characterized by warm body temperatures. Dwarf titanosaurs may have exhibited similar body temperatures to larger sauropods, although this conclusion is provisional, given current uncertainties in taxonomic assignment of dwarf titanosaur eggshell. Our results nevertheless reveal that metabolically controlled thermoregulation was the ancestral condition for Dinosauria.

## INTRODUCTION

Determining the metabolic rates of dinosaurs has remained a persistent challenge ever since the name "Dinosauria" was first coined in the 19th century (*1*). Arguments for and against dinosaurian endothermy have been made on the grounds of paleohistology, biophysical models, and isotopic signatures of fossil teeth and eggshell (*2–6*). Recent histological work has suggested that the dinosaur endothermy versus ectothermy debate is a false dichotomy and argues instead that most nonavian dinosaurs exhibited an intermediate "mesothermic" thermoregulatory strategy (*4*). However, the correlation between metabolic rate and parameters such as body mass and growth rate in extinct dinosaurs relies on loosely constrained assumptions about growth constants, scaling relationships, and the activation energy controlling biochemical reactions, which are often derived from extant reptiles and mammals and are used in modeling dinosaur metabolic rates (*2*). Variations in assumed model parameters can produce large deviations in temperature estimates (2° to 8°C), even in extant taxa (*7*). This uncertainty requires independent constraints on internal body temperatures from dinosaur fossils representing a broad range of sizes and taxonomic groups.

Carbonate clumped isotope paleothermometry (reported as $\Delta_{47}$) is based on the internal order of $^{13}C$ and $^{18}O$ atoms among C—O bonds within a carbonate mineral lattice, reflecting mineral formation temperature independent of the isotopic composition of the water from which the mineral formed (*8*). This method accurately reflects the body temperatures of living vertebrates when applied to biogenic carbonates in tooth bioapatite from reptiles, sharks, and mammals, as well as eggshell carbonate from living reptiles and birds (*6*, *9*). With this foundation, $\Delta_{47}$ paleothermometry provides a means to assess the body temperatures of nonavian dinosaurs, alleviating problematic assumptions inherent to estimating tempera-

tures from the $\delta^{18}O$ of skeletal or dental material or through the relationship of growth rate and body temperature (*4*, *10*). Previous $\Delta_{47}$-based estimates of body temperatures derived from fossil tooth enamel and eggshell of sauropods (*Camarasaurus*, *Giraffitdan*, and an unspecified titanosaur) yielded estimates in the range of 35° to 38°C (*5*, *6*), and those from oviraptorid theropod fossil eggshell yielded body temperature estimates of 32° ± 3°C (*6*). These body temperature estimates for enormous sauropods (which ranged in size from ~$10^4$ to $10^5$ kg) (*11*) fall within the range of living endotherms (*12*), whereas those for the much smaller oviraptorid (~100 kg) overlap with the body temperatures of living ectothermic and endothermic vertebrates (*6*).

Although long-standing consensus regarding the higher-order phylogenetic relationships of dinosaurs has recently been challenged (*13*), Dinosauria is unequivocally subdivided into three major clades: Sauropodomorpha, Theropoda, and Ornithischia (Fig. 1) (*13*, *14*). To date, $\Delta_{47}$ paleothermometry has never been applied to ornithischian dinosaurs, which represent either the sister taxon to all other dinosaurs (and thus the most distant dinosaurian relatives of birds) (*14*) or the sister taxon to theropods (*13*). Furthermore, studies applying $\Delta_{47}$ paleothermometry to dinosaurs have yet to control for the paleoenvironmental temperatures at which these animals lived, limiting robust metabolic interpretations. Namely, existing studies have focused on samples from low to mid (~30° to 45°) paleolatitudes, where ambient summer temperatures could have been as high as the body temperature estimates of the dinosaurs studied, thereby resulting in uncertainty with respect to thermoregulatory interpretations. For example, eggshell samples from the ectothermic-radiated tortoise (*Astrochelys radiata*) and bearded lizard (*Pogona barbata*) taken from the Los Angeles Zoo yielded temperatures within the range of living endotherms only because they came from a warm environment (*6*). Here, we apply $\Delta_{47}$ paleothermometry to assess the phylogenetic distribution of elevated core body temperatures across Dinosauria, with samples spanning the dinosaurian phylogeny (Fig. 1). Specifically, we investigate the hadrosaurid ornithischian *Maiasaura peeblesorum*, the paravian theropod *Troodon formosus* (the Mesozoic dinosaur most closely related to birds yet assessed using $\Delta_{47}$ paleothermometry; Fig. 1), and an eggshell potentially attributable

[1]Department of Geology and Geophysics, Yale University, New Haven, CT 06511, USA. [2]Department of Earth Sciences, University of Cambridge, Cambridge CB2 3EQ, UK. [3]Department of Geoscience, University of Calgary, Calgary, Alberta T2N 1N4, Canada. [4]Royal Tyrrell Museum of Palaeontology, Drumheller, Alberta T0J 0Y0, Canada. [5]Institute of Earth Sciences, The Hebrew University of Jerusalem, Jerusalem, Israel.
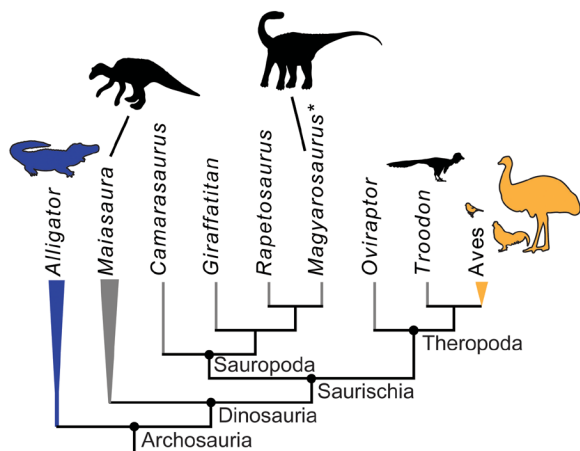\*Corresponding author. Email: robin.dawson@yale.edu

**Fig. 1. Simplified archosaur phylogeny illustrating the taxa investigated in this and previous clumped isotope studies.** Extant ectotherms are blue; extant endotherms are orange. *Maiasaura* represents the major dinosaurian subclade Ornithischia, which is traditionally thought to represent the sister taxon to a Theropoda + Sauropoda clade as shown in (14) but in some recent phylogenies is placed as sister to Theropoda (13). Asterisk indicates taxonomic uncertainty for the Romanian eggshell sample, which may derive from a titanosaur sauropod (either the dwarf taxa *Magyarosaurus* or *Paludititan* or a larger titanosaurian) or the dwarf hadrosauroid *Telmatosaurus* (39).

to a "dwarf" titanosaur sauropod from Romania (see taxonomic discussion of this eggshell in Results).

Since extant endotherms—especially large-bodied ones—are often "thermal mosaics," with their extremities approaching environmental temperatures while retaining a warmer core (10), temperature estimates from eggshells that developed near the center of a dinosaur's body are likely to be more reliable than estimates from tooth enamel. $\Delta_{47}$ estimates of body temperatures for American alligators (*Alligator mississippiensis*) and Nile crocodiles (*Crocodylus niloticus*) were 1° to 3°C warmer and closer to expected temperatures when measured from the eggshell versus tooth bioapatite (6, 9). Here, we compare dinosaurian core body temperature estimates from fossil eggshells to paleoenvironmental temperatures by using $\Delta_{47}$ paleothermometry of co-occurring ectothermic fossil mollusks or other climatic paleo-temperature estimates derived from published literature. Most of our samples come from high paleolatitude sites (Alberta, Canada), where cooler ambient temperatures facilitate linking of warm body temperature to endothermic-like metabolisms.

### Geologic and climatic setting of fossil eggshell
Eggshell fragments of *T. formosus*, *M. peeblesorum*, *Hypacrosaurus stebingeri*, and an indeterminate lambeosaurine hadrosaur (15) were recovered from the Upper Campanian (~75 million years old) Oldman Formation of southern Alberta (localities: Devil's Coulee, Wann's Hill, Lost River Ranch; fig. S1). The relatively high paleolatitude of southern Alberta (~55°N; fig. S2) (16) facilitates our investigation of thermoregulation because the difference between environmental temperature estimates and endothermic body temperatures should be great enough to be analytically distinguishable by $\Delta_{47}$ measurements. Upper Campanian mean annual temperature (MAT) estimates at 55°N, based on fossil leaf temperature proxies and $\delta^{18}O_{phosphate}$ from vertebrate fossils (teeth, turtle shell, and fish scales), are ~12° to 13°C (17, 18).

In addition, we analyzed a fossilized eggshell from the Maastrichtian (~69 million years old) Densuş-Ciula Formation of the Haţeg Basin (Southern Carpathians, Romania), a subtropical island (23°N paleolatitude) (19) within the Tethys Ocean (fig. S2). MAT estimates at this paleolatitude are variable, but range from ~30°C based on climate models (20, 21) to 18° to 25°C based on fossil leaf proxies (17) and ~25°C from $\delta^{18}O_{phosphate}$ of vertebrate fossils (teeth, turtle shell, and fish scales) (18).

## RESULTS
### $\Delta_{47}$ temperature calibration
Extant eggshell samples were analyzed to corroborate previous work (6), suggesting that modern bird and nonavian reptile eggshell carbonate $\Delta_{47}$ values reflect internal body temperatures. For birds, internal body temperatures are largely controlled by metabolism (12). Extant bird eggshell samples were obtained from personal collections or through the Yale Peabody Museum's (YPM's) Ornithology Collection. Eggshells come from the following species: emu (*Dromaius novaehollandiae*; collected in 2012 at the Songline Emu Farm in Gill, MA), chicken (*Gallus gallus*; collected in 2012 in New Haven, CT), house sparrow (*Passer domesticus*; YPM collections uncatalogued), house wren (*Troglodytes aedon*; YPM collections uncatalogued), and Ruby-throated hummingbird (*Archilochus colubris*; YPM ORN 132487). The resting body temperatures for the birds used for the $\Delta_{47}$ temperature calibration (Fig. 2) are from (22). Extant American alligator eggshell (*A. mississippiensis*; YPM HERR 015203) was collected from the Rockefeller State Wildlife Refuge (RSWR) in Grand Chenier, LA, in June 2004. Studies of American alligators from the RSWR in June and July 2001 show that alligator body temperatures closely follow environmental temperatures (23). Environmental temperatures for June 2004 when the specific alligator egg was collected averaged 27.1°C and ranged between 23.3° and 30.9°C based on local temperature gauges (24). This average environmental temperature for June 2004 is used in the $\Delta_{47}$ temperature calibration (Fig. 2). The $\Delta_{47}$ values obtained for the hummingbird, wren, and sparrow are higher than expected based on their measured body temperatures, possibly related to facultative hypothermia, a mechanism used by small birds to conserve energy during breeding. Facultative hypothermia has been documented in several bird lineages including Passeriformes (which include wrens and sparrows) and Trochilidae (hummingbirds) (25). Our modern eggshell $\Delta_{47}$ values show good agreement with previous modern eggshell calibrations obtained from other laboratories (6), as well as a laboratory precipitation calibration from (8), which was generated in the same laboratory following the same analytical protocol as our eggshell data (Fig. 2).

It has been suggested recently (26) that the isotopic parameters used to estimate $^{17}O$ abundance, as part of the calculation of $\Delta_{47}$, require revision. Currently, the preferred method for calculating $\Delta_{47}$ uses the "Brand parameters" as opposed to those originally used (termed "Gonfiantini parameters"). However, when converting the Yale biogenic carbonate $\Delta_{47}$ values and the laboratory-precipitated carbonate data from (8) to the Brand parameters, the $\Delta_{47}$ values show contrasting responses (fig. S3). The result is a mismatch between biogenic and laboratory precipitation $\Delta_{47}$ temperature calibrations, which is unexpected given previous agreement between them (Fig. 2). Generally, for samples with $\delta^{13}C$ and $\delta^{18}O$ similar to that of the reference gas, the choice of $^{17}O$ isotopic parameters exerts only a small effect on $\Delta_{47}$. However, the laboratory precipitation
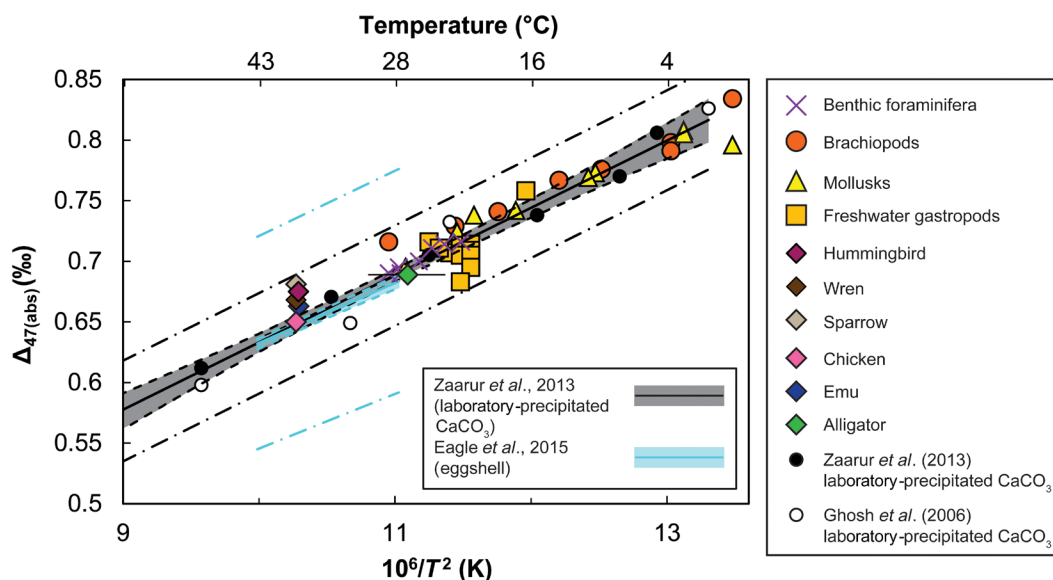
**Fig. 2. Clumped isotope [$\Delta_{47(abs)}$] value (calculated using the Gonfiantini parameters) versus temperature relationship of extant eggshell.** Data from this study, other biogenic carbonates analyzed between 2010 and 2018 at Yale University (8, 56–59), the calibration of laboratory precipitated carbonates from (8), and the extant eggshell carbonate calibration from (6). Error bars are SE for $\Delta_{47}$ (smaller than the symbols) and the range of expected body temperatures. Calibration lines, solid line; 95% confidence error envelope, shaded line; and 95% prediction envelope, dashed-dotted lines.

samples used to generate the $\Delta_{47}$ temperature calibration in (8) are much more depleted in $^{13}$C [$\delta^{13}$C of ~−30‰ Vienna Pee Dee Belemnite (VPDB)] compared with biogenic carbonates and the reference gas ($\delta^{13}$C of −3.640‰ VPDB). Therefore, the difference in behavior of the biogenic and laboratory precipitation samples is probably due to uncertainty in the retroactive conversion process from the Gonfiantini to the Brand parameters, related to the fact that the standards used for defining the absolute reference frame (see the Supplementary Materials for more details) were not designed for this conversion. It is likely that the $^{13}$C-depleted laboratory precipitation data are more sensitive to this uncertainty. Resolving some of this uncertainty could be achieved by repeating the laboratory precipitation experiments from (8) to produce synthetic carbonates with a range of different carbon isotope compositions.

Because of remaining questions regarding the conversion process to Brand parameters and its effect on older Gonfiantini-calculated $\Delta_{47}$ data, we used three possible $\Delta_{47}$ temperature calibrations to estimate temperature from our Brand parameter $\Delta_{47}$ data (see the Supplementary Materials for more details). When using any one of these three equations, the difference in temperature is on average less than 1°C relative to the results obtained using the original Gonfiantini parameters and the calibration from (8) (data S1). We therefore report our data using the Gonfiantini parameters and the Gonfiantini-based $\Delta_{47}$ temperature calibration (Fig. 2) from (8), as it is in agreement with our biogenic data and enables direct comparisons with previously published dinosaur body temperature estimates (5, 6).

**Preservation of fossil carbonates**

Before making any interpretation of dinosaur body temperature based on $\Delta_{47}$ paleothermometry results, we must consider the preservation of the fossil carbonates. The internal order of $^{13}$C—$^{18}$O bonds within the mineral lattice may change during burial diagenesis or due to recrystallization (27), altering $\Delta_{47}$ signatures such that the derived

temperatures may reflect the temperature of recrystallization rather than the original environmental or body temperature of carbonate formation. To account for this potential limitation, we first assessed the degree of eggshell preservation by examining the eggshell morphology and identifying any nonprimary eggshell microstructures. All fossil eggshells were imaged using a scanning electron microscope and a petrographic microscope to assess preservation of primary eggshell microstructure. Biogenic carbonates that retain fine microstructure are more likely to preserve the original mineral and therefore their original geochemical signatures, as recrystallized calcite often loses the preferential orientation of biosynthesized crystals (28). Next, we analyzed fossil carbonate for evidence of recrystallization using trace element concentrations and cathodoluminescence (CL) microscopy. In addition, we used x-ray diffraction to assess the preservation of the original aragonite in mollusk shell fossils. See Table 1 for summary of results.

**Morphology of eggshells**

Accurate taxonomic identification of fossil eggshell is fundamental to understand the evolutionary implications of dinosaur body temperatures when using eggshell carbonate $\Delta_{47}$ values. Although classification of dinosaur eggshell may be complicated by a lack of association with identifiable skeletal material, eggshell can be diagnosed much like skeletal morphology for taxonomic assignment (29). The eggshell of *T. formosus* (ootaxon *Prismatoolithus levis*) (30) has been identified based on eggs containing embryonic remains from the Campanian Two Medicine Formation of Montana (31). *Troodon* eggshell is about 1 mm thick, has a smooth outer surface with single- and double-pore openings, and consists of two main layers representative of the continuous/prismatic and mammillary zones of nonavian theropod dinosaurs (32). In the three *Troodon* samples, this diagnostic eggshell bilayer is well preserved (Fig. 3, A to C). On the basis of the primary eggshell structure, the *Troodon* samples pass the first criterion of being well preserved (Table 1). The excellent

**Table 1. Criteria for characterization of fossil eggshell preservation.**

| Eggshell | Locality | Mn (ppm) | Fe (ppm) | CL image % luminescent | Preservation test* | | | | Final preservation characterization |
|---|---|---|---|---|---|---|---|---|---|
| | | | | | Low-trace metals | % Lum. | Microstructure | 1° Aragonite | |
| *Troodon formosus* (Theropod) TMP 2008.75.127 | Devil's Coulee, AB, Canada | 60[†] | 76[†] | 0.5 | ✓✓ | ✓✓ | ✓✓ | NA | Well preserved |
| *Maiasaura peeblesorum* (Hadrosaur) TMP 2009.153.1 | Devil's Coulee, AB, Canada | 1560 | 741 | 11.3 | ✓ | ✓ | ✓✓ | NA | Moderately preserved |
| *Hypacrosaurus stebingeri* (Hadrosaur) TMP 1989.69.10 | Devil's Coulee, AB, Canada | 4291[†] | 2313[†] | NA | X | NA | NA | NA | Poorly preserved |
| *Troodon formosus* (Theropod) TMP 1995.21.4 | Wann's Hill, AB, Canada | 99 | 54 | 0.6 | ✓✓ | ✓✓ | ✓✓ | NA | Well preserved |
| Indeterminate lambeosaurine (Hadrosaur) TMP 1988.121.41 | Wann's Hill, AB, Canada | 3265 | 1623 | 73 | X | X | X | NA | Poorly preserved |
| *Troodon formosus* (Theropod) TMP 2003.81.1 | Lost River Ranch, AB, Canada | 62 | 8 | 0 | ✓✓ | ✓✓ | ✓✓ | NA | Well preserved |
| *Magyarosaurus dacus* (Sauropod) TMP 1991.175.2 | Tuştea, Haţeg Basin, Romania | 795 | 6 | 15 | ✓ | ✓ | ✓✓ | NA | Moderately preserved |
| Gastropod W20 | Wann's Hill, AB, Canada | 79 | 297 | NA | ✓✓ | NA | NA | ✓✓ | Well preserved |
| Bivalve TMP 2009.149.5 | Milk River, AB, Canada | 218 | 21 | NA | ✓✓ | NA | NA | ✓✓ | Well preserved |

*If the sample passed, it received a "✓✓"; partially passed, a "✓"; or failed, a "X." NA indicates that either test was "not applicable" (e.g., original biomineral was calcite) or "not available" (e.g., no thin sections available).    †Average of duplicates run to test stability of mass spectrometer.

preservation of the *Troodon* microstructure could be due to the fact that these shells are the least porous of all the taxa examined here, possibly limiting exposure to pore fluids that may cause calcite dissolution and reprecipitation.

The eggshell diagnostic of *M. peeblesorum* (ootaxon *Spheroolithus albertensis*) (33) is over 1 mm thick and has a surface ornamentation of anastomosing ridges, irregular pore canals, and fan-shaped shell units with radiating tabular structure (Fig. 3D) (29, 33). Association between the hadrosaur *Maiasaura* and the ootaxon *S. albertensis* is based on hatchling skeletal material found in association with eggs and eggshells from the Campanian Two Medicine Formation of Montana (15). The *Maiasaura* eggshell is more porous than that of *Troodon* (Fig. 3), and coarse-grained calcite infilling is observed in the pore canals. However, the diagnostic microstructure of radiating tabular basic units is preserved, suggesting that the majority of the eggshell calcite is primary mineral, with relatively minor amounts of secondary calcite (Fig. 3D and Table 1; see below for a quantitative discussion).

Determination of the taxonomic affinity of the eggshell from Romania (ootaxon *Megaloolithus* cf. *Megaloolithus siruguei*) (34) is more complicated. Characteristics of the Romanian eggshell include nodular surface ornamentation, Y-shaped vertical pore canals, and fan-shaped shell units composed of acicular calcite crystals radiating from nucleation centers (Fig. 3E). These features are shared by fossil eggs

from Auca Mahuevo, Argentina, which can be confidently identified as belonging to titanosaur sauropods based on embryos in ovo (within the egg) (35). Compatible with a titanosaur affinity for the Romanian eggs, skeletal material from two dwarf titanosaur species (the similarly sized *Paludititan nalatzensis* and *Magyarosaurus dacus*) (36, 37) and one indeterminate, large titanosaur species (38) have been recovered from the Haţeg Basin. Although multiple eggshell characteristics are compatible with a titanosaur affinity, embryonic remains of the dwarf hadrosauroid *Telmatosaurus* have also been recovered within the Haţeg Basin, in close proximity to a *Megaloolithus* cf. *M. siruguei* nest (39, 40). This has prompted the idea that *Telmatosaurus* may have convergently evolved oological characteristics such as those in sauropods, raising uncertainty of a titanosaur affinity for this Romanian eggshell (39, 40). For the purpose of this study, if these eggshells derive from the dwarf hadrosauroid *Telmatosaurus*, then they provide additional information on ornithischian body temperatures. However, given its numerous similarities with eggshell associated with definitive titanosaur embryos from Argentina, we consider it most plausible that these eggshells are from Romanian titanosaurs, either dwarf or giant. However, since the taxonomic identification of the eggshells is not yet definitive, we discuss the implications of both a hadrosauroid and titanosaur affinity for these eggshells.

Fossil bone histology (37) suggests that the dwarf titanosaurs of Romania had an adult body mass of ~900 kg—at least an order of
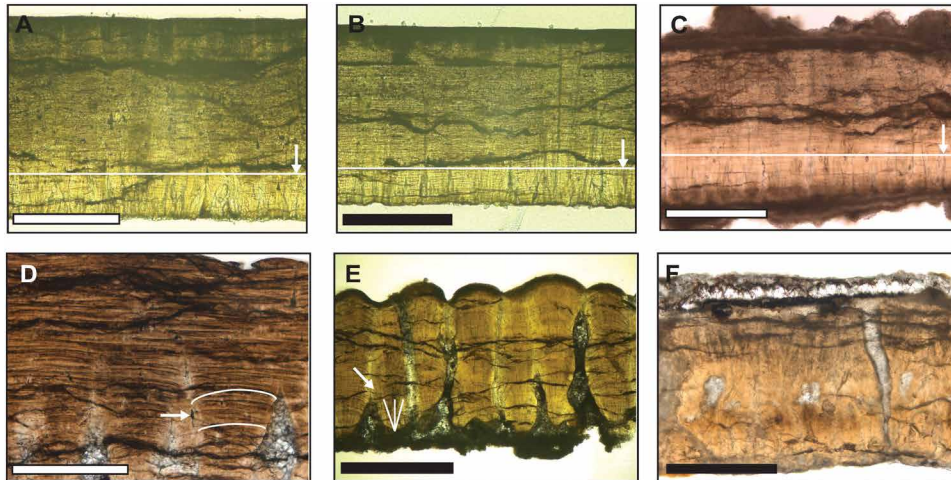
**Fig. 3. Petrographic microscope images of dinosaur eggshell from this study.** (**A**) Well-preserved *Troodon* eggshell from Devil's Coulee, Alberta, Canada [Tyrrell Museum of Palaeontology (TMP) 2008.75.51]. (**B**) Well-preserved *Troodon* eggshell from Lost River Ranch, Alberta, Canada (TMP 2003.81.1). (**C**) Well-preserved *Troodon* eggshell fragment from Wann's Hill, Alberta, Canada (TMP 1995.21.4). Arrows and horizontal lines point to the approximate boundary between the mammillary and prismatic layers. Presence of two calcitic layers is diagnostic of nonavian theropods. (**D**) *Maiasaura* hadrosaur eggshell from Devil's Coulee, Alberta, Canada, with intermediate preservation (TMP 2009.153.1). The diagnostic radiating tabular units are indicated by the white arrow. (**E**) Romanian eggshell (oospecies *Megaloolithus* cf. *M. siruguei*, TMP 1991.175.2) from Tuştea locality, Romania, with intermediate preservation. Diagnostic radiating acicular crystals indicated by white arrow. (**F**) Poorly preserved lambeosaurine hadrosaur eggshell fragment from Wann's Hill, Alberta, Canada (TMP 1988.121.41). Scale bars, 500 μm.

magnitude smaller than titanosaurs from Argentina. In turn, the body length of *Telmatosaurus* is estimated to have been ~4 m, compared to the 7- to 13-m (or more) body lengths of most hadrosaurids (*41*). The relatively small size of these Romanian dinosaurs has been interpreted as evidence of island dwarfism, as the Haţeg Basin would have been located on an island in the Tethys during the Maastrichtian (*19*).

The Romanian eggshell is also porous, with diagnostic "Y-shaped" pore canals, which appear to have been filled with secondary calcite (Fig. 3E). The preservation of the primary acicular radiating calcite crystals from the nucleation centers indicates that the majority of the original eggshell calcite is preserved. The volume of secondary calcite that could fill these pore spaces is small relative to the total eggshell calcite volume (Fig. 3E; see below for a quantitative discussion).

Hadrosaur eggshells from two Alberta localities (*H. stebingeri* eggshell from Devil's Coulee and indeterminate lambeosaurine eggshell from Wann's Hill; see the Supplementary Materials for more details about geologic settings) display obvious secondary calcite overgrowths on their exterior and have lost or partially lost their original microstructure (e.g., Fig. 3F). We therefore consider these samples as poorly preserved (Table 1).

### Mollusk Shell preservation

In contrast to dinosaur eggshell carbonate, which is composed of calcite, freshwater mollusk shells are originally composed of aragonite. The Wann's Hill gastropod and Milk River bivalve mineral preservation was assessed using x-ray diffraction (fig. S4), which shows clear aragonite peaks and no calcite peaks, suggesting that these mollusk samples are well preserved and are therefore considered adequate for environmental temperature determination from isotopic analysis (Table 1). This conclusion was further tested using trace element analysis on both mollusk and eggshell samples.

### Trace element analysis

Trace elements, such as Fe and Mn, are not common in eggshells of living taxa but are typically present in anoxic pore fluids in which calcite eggshell may recrystallize during diagenesis (*28*). Bulk concentrations of trace metals were measured in eggshell and mollusk carbonates as indicators of recrystallization and therefore likely alteration of $\Delta_{47}$ values. Mn concentrations in the eggshells from extant taxa were below detection limits. Fe concentrations were 5 parts per million (ppm) for extant chicken, sparrow, and alligator eggshell, and below detection limit in extant emu eggshell. Concentrations of Fe and Mn in the fossil eggshell were between ~50 and 80 ppm Fe and ~60 and 100 ppm Mn for the best-preserved samples (the three *Troodon* eggshell samples), and between ~1500 and 2500 ppm Fe and 1500 and 4500 ppm Mn for obviously altered hadrosaur eggshell based on their poorly preserved microstructure (Devil's Coulee *Hypacrosaurus* and Wann's Hill lambeosaurine; Table 1 and Fig. 4A). Two eggshell samples (*Maiasaura* and the Romanian eggshell) exhibited intermediate trace metal concentrations of ~0 to 750 ppm Fe and 800 to 1600 ppm Mn (Table 1 and Fig. 4A). See the Supplementary Materials for more details.

### CL microscopy

This technique was used to characterize fossil eggshell preservation by identifying the extent of diagenetic calcite overgrowth, infilling, and replacement of the original mineral. CL microscopy identifies areas within the shell that are enriched in Mn and Fe: regions enriched in Mn luminesce, and when subsequently enriched in Fe, these areas become dimmer (*28*).

CL photomicrographs of *Troodon* eggshell samples in thin section are nonluminescent (Fig. 4B and fig. S5, G to I), consistent with their low bulk concentrations of Fe and Mn (Fig. 4A) and their preservation of primary eggshell microstructure (Fig. 3, A to C). We therefore characterize the *Troodon* eggshells as well preserved (Table 1) and appropriate for body temperature determination from isotopic analysis. In contrast, the Wann's Hill lambeosaurine, in which microstructure was not preserved, was luminous throughout (Fig. 4E), likely due to both high Fe and Mn concentrations (Fig. 4A). The lambeosaurine eggshell was characterized as poorly preserved (Table 1) and inappropriate for body temperature determination from isotopic analysis.
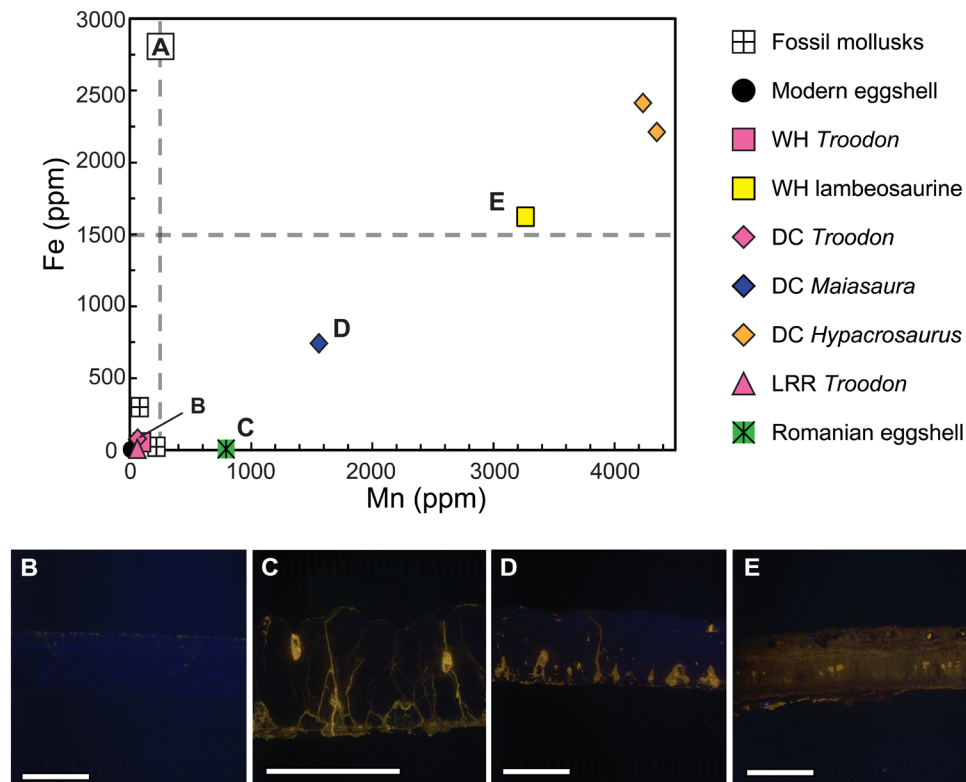
**Fig. 4. Bulk trace metal concentrations in eggshells and mollusks with CL images of fossil eggshell.** (**A**) Fe and Mn concentrations (ppm) in extant and fossil eggshells and fossil mollusks. Letters in the graph refer to specific CL images. (**B** to **E**) CL images of fossil eggshell thin sections in cross section used to assess preservation. (B) Well-preserved Devil's Coulee *Troodon*, (C) Romanian eggshell (oospecies *Megaloolithus* cf. *M. siruguei*) with intermediate preservation, (D) *Maiasaura* from Devil's Coulee with intermediate preservation, (E) poorly preserved lambeosaurine from Wann's Hill, Alberta, Canada. Scale bars, 1 mm. Luminescence correlates with increased Mn concentrations in (A).

The Devil's Coulee *Maiasaura* eggshell sample exhibits well-preserved microstructure (Fig. 3D) but contains minor amounts of secondary calcite and moderately elevated Fe and Mn concentrations (Fig. 4A). This sample had bulk nonluminescent calcite but luminescent calcite filling in thin cracks and pores, consistent with secondary calcite infilling being the source of Mn and Fe (Fig. 4D). This Mn and Fe content could also be what gives the eggshell its black color. It is likely that the $\Delta_{47}$ value reflects a mixture of original eggshell (and therefore actual dinosaur body temperature), with a minor contribution of diagenetic secondary calcite, which in turn reflects ambient or burial temperatures. The Romanian eggshell sample also exhibits well-preserved microstructure (Fig. 3E) with minor secondary calcite filling in cracks and pores (Fig. 4C) and only moderately elevated Mn concentrations (Fig. 4A).

The CL images (Fig. 4, B to E, and fig. S5) can be used to quantify the contribution from secondary calcite. Since luminescent areas are indicative of trace metal enrichment and, thus, likely areas of recrystallization, we used the number of luminescent pixels to estimate the fraction of the eggshell that is recrystallized (see the Supplementary Materials for more details). For the *Maiasaura* eggshell, we estimate ~11% is recrystallized, and for the Romanian eggshell, ~16% is recrystallized (Table 1). On the basis of well-preserved microstructure and relatively low amounts of recrystallized calcite, we characterize the *Maiasaura* and Romanian eggshell as moderately preserved (Table 1) and adequate for body temperature determination from isotopic analysis.

## Dinosaur body temperatures

The theropod *Troodon* eggshells yielded average (± 1 SE) $\Delta_{47}$-derived temperatures of 38° ± 4°C, 27° ± 4°C, and 28° ± 3°C, and the ornithischian *Maiasaura* eggshell yielded a temperature of 44° ± 2°C (Fig. 5). The $\Delta_{47}$-derived temperature obtained from the Romanian eggshell producer is 36° ± 1°C. This is within the range of living endothermic animals, such as birds and mammals (34° to 44°C) (*12*) and is warmer than the modeled MAT for the Haţeg Basin locality of ~30°C (*20*, *21*). The warmest *Troodon* (38° ± 4°C) and *Maiasaura* (44° ± 2°C) body temperature estimates are also within the range of living endothermic animals and substantially exceed the warmest environmental temperatures estimated from mollusk shells at the same location (25° ± 1°C and 28° ± 2°C; Fig. 5).

## DISCUSSION

The $\Delta_{47}$-derived mollusk temperatures provide a direct way for comparing dinosaur body temperature estimates to that of their environment and determine whether these dinosaurs had thermo-regulatory strategies closer to modern endothermic or ectothermic animals. Considering the highly seasonal growth of extant mid-high-latitude freshwater bivalves and gastropods (*42*), these environmental temperatures likely reflect the warm season. Mann-Whitney tests were conducted to compare dinosaurian body temperatures to average mollusk-derived environmental temperatures. These tests indicate that the *Maiasaura* and Devil's Coulee *Troodon* temperatures
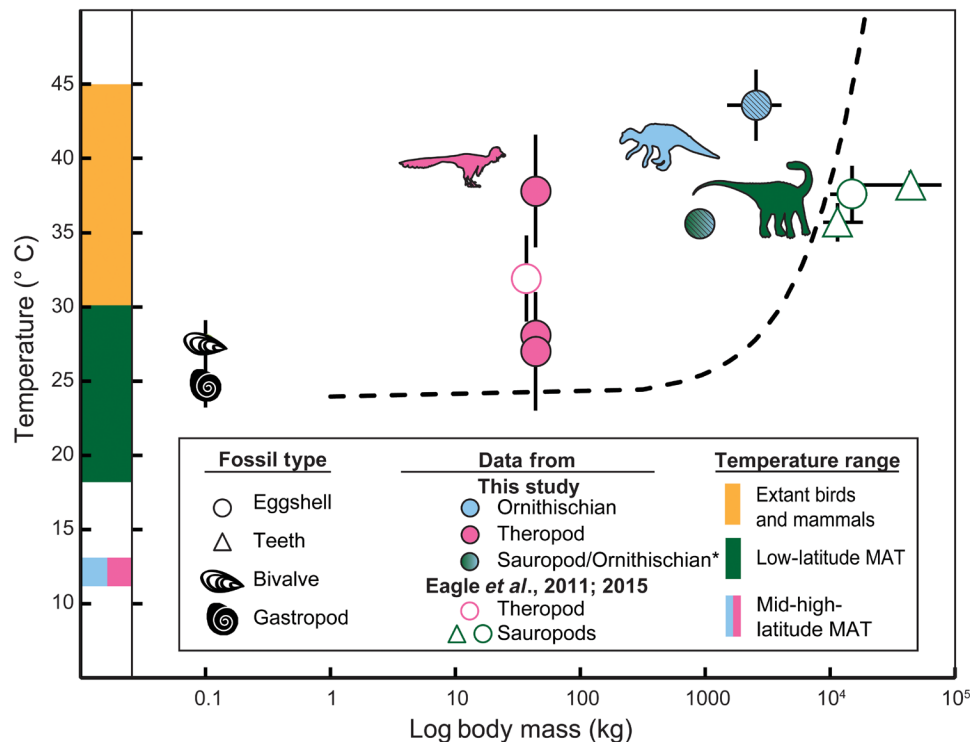
**Fig. 5. Log body mass (kg) versus $\Delta_{47}$-derived body temperature estimates of fossil dinosaurs and mollusks.** We present data from this study and (5, 6) in the context of model-based body temperature estimates from (2) (black dashed curve). Note that this model provides an illustrative example for the possibility of gigantothermy, but it has been debated (7). Diagonal-hatched symbols are specimens with moderate calcite preservation, while the rest are well preserved. Estimates of ambient MAT are taken from the literature (17, 18, 20, 21) for the latitudes of Late Cretaceous sites in Haţeg Basin, Romania (green bar), and Alberta, Canada (blue/pink bar). For Alberta, ambient warm season temperatures are also estimated from $\Delta_{47}$ in freshwater mollusks (shell symbols). $\Delta_{47}$ temperature error bars are 1 SE, and body mass error bars indicate a range of estimated sizes (11, 37, 60). Extant bird body temperature range is from (12). Asterisk indicates taxonomic uncertainty for the Romanian eggshell sample, which may derive from a titanosaur sauropod or the hadrosauroid *Telmatosaurus* (39).

are both significantly warmer than the mollusk temperatures ($U_b = 0$, $P = 0.0024$, and $U_b = 6$, $P = 0.0363$). By contrast, the two cooler *Troodon* samples [Lost River Ranch (27° ± 4°C) and Wann's Hill (28° ± 3°C)] yield estimates similar (i.e., not significantly different) to the estimated summer environmental temperatures of fossil mollusk shells from the same deposits ($U_b = 8$, $P = 0.3196$, and $U_b = 17$, $P = 0.5953$; Fig. 5). Although these estimates are consistent with those previously obtained for a Mongolian oviraptorid (32° ± 3°C) (6), the ~10°C range of body temperatures within these three Alberta *Troodon* samples may suggest a capacity for heterothermic metabolism (Fig. 5) (43).

The *Maiasaura* eggshell is not as well preserved as the *Troodon* eggshells (~11% recrystallization or infilling of secondary calcite in the *Maiasaura* sample). Consideration of several possible diagenetic scenarios allows us to assess the potential effect of this secondary calcite on $\Delta_{47}$ using a simple mass balance. Under one scenario, the secondary calcite could have formed from diagenetic fluids after burial. On the basis of vitrinite reflectance data from southern Alberta, the burial temperatures were likely below 80°C (44). Assuming that $\Delta_{47}$ of the secondary calcite reflects a formation temperature of at most 80°C, this would correspond to a $\Delta_{47}$ value of 0.523‰. If this estimated 11% of secondary calcite is mixed with the remaining 89% primary calcite to yield the combined measured $\Delta_{47}$ of 0.632‰, then we can use a simple two end-member mixing model to estimate the primary unaltered calcite $\Delta_{47}$ as 0.645‰. This corresponds to a body temperature of 40°C. Thus, the effect of recrystallized calcite

under this scenario does not change our biological interpretation, as the estimated *Maiasaura* body temperature still falls within the range of extant endotherms.

A second possible burial scenario for the *Maiasaura* is that of surface diagenesis, in which recrystallized calcite formed from diagenetic fluids before burial and reflects temperatures close to ambient (~26°C, $\Delta_{47}$ 0.698‰, based on our average freshwater mollusks $\Delta_{47}$). Similar mass balance considerations result in $\Delta_{47}$ of 0.623‰ for the primary calcite, corresponding to a body temperature of 46°C. Another option for a surface diagenesis scenario is to use the clearly altered *Hypacrosaurus* fossil from the same locality (Devil's Coulee), with very high trace metal concentrations (Fig. 4A), as the end member for total recrystallization at this site. Hence, a 100% recrystallized shell yields $\Delta_{47}$ of 0.681‰ (same as the *Hypacrosaurus*). Mass balance calculations then result in primary calcite being 0.625‰ with a corresponding body temperature of 45°C. Under these two surface diagenesis scenarios, our *Maiasaura* body temperature estimate of 44°C is a minimum temperature. The diagenetic history probably involved some dissolution and reprecipitation at the surface and some at depth, but either way, the impact of any secondary calcite on our biological interpretation is minimal.

In addition to dissolution and reprecipitation or pore infilling by secondary calcite due to interactions with diagenetic fluids, it is possible that $\Delta_{47}$ temperatures in *Maiasaura* were affected by solid-state reordering due to burial heating. To rule out this possibility, we

compared the *Maiasaura* sample with poorly preserved *Hypacrosaurus* eggshell fossils from the same locality. The *Hypacrosaurus* eggshell experienced the same thermal history during burial as the *Maiasaura* eggshell but yielded a $\Delta_{47}$ temperature estimate of ~30°C—much lower than that of the *Maiasaura* eggshell ($\Delta_{47}$ temperature estimate of ~44°C). While these samples clearly experienced different extents of recrystallization as discussed above, it is unlikely that burial heating would have initiated solid-state reordering in the *Maiasaura* eggshell but not in that of *Hypacrosaurus*. Thus, these results support the use of isotopic temperatures from the *Maiasaura* eggshell to infer body temperatures, which in turn suggests their capacity for metabolic thermoregulation.

The Romanian eggshell is derived either from the dwarf hadrosauroid *Telmatosaurus* or from a titanosaur sauropod. This eggshell yielded a $\Delta_{47}$-derived temperature of 36° ± 1°C (Fig. 5). Preservation quality is a consideration also when interpreting body temperatures estimated from the Romanian eggshell. This specimen has slightly elevated Mn concentrations, likely from secondary calcite pore infilling, as indicated by luminous areas on photomicrographs (~16% of the material; Fig. 4C). The Maastrichtian Densuş-Ciula Formation was buried under as little as 500 m of overlying sediment for the past 65 million years (45). With an average geothermal gradient of ~25°C/km (46) and assuming the maximum MAT of 30°C (20, 21), the burial temperature would be 42.5°C. This gives a primary calcite $\Delta_{47}$ value of 0.665‰ (using similar mass balance considerations as those for *Maiasaura*, above) and a corresponding body temperature estimate of 34°C in a burial diagenesis scenario. Alternatively, using the MAT of 30°C (20, 21) as the surface diagenetic temperature, the primary calcite $\Delta_{47}$ value would be 0.656‰ and correspond to a body temperature of 37°C. Under both scenarios, the change is small and does not affect our biological interpretation.

The presence of rare large-bodied sauropod remains in the Haţeg Basin precludes the definitive assignment of the Romanian eggshell to a dwarf titanosaur. However, remains of the dwarf taxa *Magyarosaurus* and *Paludititan* greatly outnumber those of large-bodied sauropods in the region (37). Hence, the implications of this eggshell deriving from one of these dwarf titanosaur taxa (either *Magyarosaurus* or *Paludititan*)—a clade composed predominantly of giant sauropods—is worth exploring. If the Romanian eggshell material is hadrosaurid in origin, then the results provide additional evidence (beyond *Maiasaura*) of ornithischian body temperatures within the range of extant birds. By contrast, if this material originates from a large titanosaur species, then the body temperature estimate of 36° ± 1°C is comparable to previous $\Delta_{47}$-derived body temperature estimates of ~35° to 38°C for giant titanosaurs, based on fossil teeth and eggshell (5, 6). If the Romanian eggshell is derived from a dwarf titanosaur, then it would allow testing of the hypothesis that the large body size of sauropods is responsible for their high body temperatures, as has previously been suggested (47). Body mass estimates for the dwarf titanosaurs of the Haţeg Basin suggest that they weighed only ~900 kg (37), much smaller than their colossal relatives ($10^4$ to $10^5$ kg) (11). The concept of "gigantothermy" or "inertial homeothermy" is based on the link between low surface area–to–volume ratios and heat retention in animals and is modeled from the relationship between body mass and temperature in living crocodilians (2), although the accuracy of this model has recently been called into question (7). If the Romanian eggshell is derived from a dwarf titanosaur,

then the similarity in body temperatures with that of giant sauropods (~35° to 38°C) (5, 6), despite an at least 10-fold difference in body mass, would be inconsistent with an inertial homeothermy thermoregulatory model (dashed curve, Fig. 5) (2). Our results from the Romanian eggshell—tentative though they are—are consistent with a recent critique of the inertial homeothermy model that suggested no relationship between size and body temperature in sauropods (7). The modeled MAT for the Haţeg Basin is ~30°C (Fig. 5) (20, 21). Seasonal models of Maastrichtian climate are not available, but a Campanian model with four times preindustrial levels of $CO_2$ gives an approximate summer temperature of ~33°C at ~23°N (48). Our body temperature estimates from the Romanian eggshell (36° ± 1°C) are warmer than either mean annual or summer paleoenvironmental temperature estimates, thus favoring an interpretation of endothermy for this eggshell producer.

Our inferred dinosaur body temperatures, combined with previous work on oviraptorosaurs and large-bodied sauropods (5, 6), indicate that representatives of all three major dinosaurian lineages exhibited elevated body temperatures relative to environmental temperatures, suggesting that a capacity for metabolic control of internal body temperatures was ancestral for Dinosauria. The variable body temperatures of *Troodon* (range of ~10°C; Fig. 5) suggest that some Mesozoic dinosaurs may have exhibited thermoregulatory strategies similar to those of extant mesothermic or heterothermic taxa. Many extant birds and mammals are heterothermic (43); they can lower their internal body temperatures to save energy during periods of environmental stress or during reproductive periods before laying eggs (43). Extant mesotherms, such as leatherback sea turtles (47), use a higher metabolism to raise their internal body temperatures above those of their surroundings but do not necessarily maintain a fixed internal body temperature such as homeothermic animals (4). Our data therefore expand on previous $\Delta_{47}$ results from theropods and sauropods in suggesting that these dinosaurs exhibited at least some metabolic control over their body temperatures to raise them above ambient temperatures, independent of their body size. *Maiasaura*, with body temperature estimates within the range of extant birds (44° ± 2°C; Fig. 5), extends this conclusion to Ornithischia.

The observed high body temperatures across all three major dinosaur clades point toward a potential decoupling of the proposed relationship between mass-specific growth rates and metabolic rates in Mesozoic dinosaurs. Although many crownward stem avians, such as *Archaeopteryx* (49), exhibited slower growth rates than extant birds, our results indicate that these extinct avian taxa would have inherited an ancestral capacity for thermoregulation. Hence, estimates of growth rates and body size may be insufficient to delineate metabolic modes in the fossil record. Heat retention scales negatively with size—a consequence of smaller animals exhibiting higher surface area–to–volume ratios than larger animals (50). Insulation would have been increasingly important throughout the protracted period of body size reduction along the evolutionary lineage toward extant birds (51, 52). Therefore, the acquisition of dense plumage among Mesozoic dinosaurs, which may have arisen independently in theropods (53) and ornithischians (54) or deeper still along the lineage subtending pterosaurs and dinosaurs (55), may have been related to selection for body heat retention in smaller-bodied animals before being co-opted for sexual display or flying potential.

## MATERIALS AND METHODS

### Trace metal analysis and CL microscopy

Extant bird, alligator, and fossil dinosaur eggshells were crushed using a mortar and pestle. Powdered samples (~6 mg each) were weighed into 1.5-ml acid-cleaned centrifuge tubes and sequentially leached with 0.35 N HCl. The combined supernatants from each leaching step were dried and redissolved in enough 5% $HNO_3$ to reach a dilution factor of 1000, along with a 2-ppb indium spike. These solutions were analyzed using a Thermo Element XR ICP-MS and compared to in-house trace element analytical standards and two geostandards with a Ca spike to match our sample solutions. CL photomicrographs of eggshell thin sections were imaged using a RELIOTRON VII CL apparatus. For more details, see the Supplementary Materials and Methods.

### Clumped isotope ($\Delta_{47}$) analysis

The clumped isotope analytical procedure at the Yale Analytical and Stable Isotopic Center is described in detail in the Supplementary Materials and Methods. Powdered carbonate samples (3.5 to 5 mg) were reacted with 105% phosphoric acid ($H_3PO_4$) overnight at 25°C. The extracted $CO_2$ was cryogenically purified on a vacuum line and passed through a gas chromatography column (Supelco Q-plot, 30 m by 0.53 mm) at −20°C to remove volatile organic compounds. Clean $CO_2$ samples were analyzed for $\delta^{13}C$, $\delta^{18}O$, and $\Delta_{47}$ using Thermo MAT-253 optimized to measure mass/charge ratio of 44 to 49. We report our $\Delta_{47}$ data using the Gonfiantini parameters in the main text and give $\Delta_{47}$ data that were calculated using the Brand parameters in the Supplementary Materials (data S1).

## SUPPLEMENTARY MATERIALS

Supplementary material for this article is available at http://advances.sciencemag.org/cgi/content/full/6/7/eaax9361/DC1

Supplementary Materials and Methods
Fig. S1. Fossil localities in southern Alberta, Canada.
Fig. S2. Paleogeographic map.
Fig. S3. Clumped isotope [$\Delta_{47(abs)}$] value versus temperature relationship of laboratory-precipitated carbonate calibration data.
Fig. S4. X-ray diffraction spectra of fossil mollusks.
Fig. S5. Photomicrographs of dinosaur eggshell samples.
Table S1. Specimen descriptions, localities, and isotopic values.
Data S1. Raw data for both carbonate samples and standards and $CO_2$ standards.
References (61–75)

## REFERENCES AND NOTES

1. R. Owen, Report on British fossil reptiles. *Rep. Brit. Assn. Adv. Sci.* **11**, 60–204 (1841).
2. J. F. Gillooly, A. P. Allen, E. L. Charnov, Dinosaur fossils predict body temperatures. *PLOS Biol.* **4**, 1467–1469 (2005).
3. R. Amiot, C. Lécuyer, E. Buffetaut, G. Escarguel, F. Fluteau, F. Martineau, Oxygen isotopes from biogenic apatites suggest widespread endothermy in Cretaceous dinosaurs. *Earth Planet. Sci. Lett.* **246**, 41–54 (2006).
4. J. M. Grady, B. J. Enquist, E. Dettweiler-Robinson, N. A. Wright, F. A. Smith, Evidence for mesothermy in dinosaurs. *Science* **344**, 1268–1272 (2014).
5. R. A. Eagle, T. Tütken, T. S. Martin, H. C. Fricke, M. Connely, R. L. Cifelli, J. M. Eiler, Dinosaur body temperatures determined from isotopic ($^{13}C$-$^{18}O$) ordering in fossil biominerals. *Science* **333**, 443–445 (2011).
6. R. A. Eagle, M. Enriquez, G. Grellet-Tinner, A. Perez-Huerta, D. Hu, T. Tütken, S. Montanari, S. J. Loyd, P. Ramirez, A. K. Tripati, M. J. Kohn, T. E. Cerling, L. M. Chiappe, J. M. Eiler, Isotopic ordering in eggshells reflects body temperatures and suggests differing thermophysiology in two Cretaceous dinosaurs. *Nat. Commun.* **6**, 8296 (2015).
7. E. M. Griebeler, Body temperatures in dinosaurs: what can growth curves tell us? *PLOS ONE* **8**, e74317 (2013).
8. S. Zaarur, H. P. Affek, M. T. Brandon, A revised calibration of the clumped isotope thermometer. *Earth Planet. Sci. Lett.* **382**, 47–57 (2013).
9. R. A. Eagle, E. A. Schauble, A. K. Tripati, T. Tütken, R. C. Hulbere, J. M. Eiler, Body temperatures of modern and extinct vertebrates from $^{13}C$-$^{18}O$ bond abundances in bioapatite. *Proc. Natl. Acad. Sci. U.S.A.* **107**, 10377–10382 (2010).
10. A. Chinsamy, J. Willem, in *The Dinosauria*, D. B. Weishampel, D. Peter, H. Osmólska, Eds. (University of California Press, 2004), pp. 643–659.
11. P. M. Sander, A. Christian, M. Clauss, R. Fechner, C. T. Gee, E. M. Griebeler, H.-C. Gunga, J. Hummel, H. Mallison, S. F. Perry, H. Preuschoft, O. W. M. Rauhut, K. Remes, T. Tütken, O. Wings, U. Witzel, Biology of the sauropod dinosaurs: the evolution of gigantism. *Biol. Rev.* **86**, 117–155 (2011).
12. A. Clarke, P. Rothery, Scaling of body temperature in mammals and birds. *Funct. Ecol.* **22**, 58–67 (2008).
13. M. G. Baron, D. B. Norman, P. M. Barrett, A new hypothesis of dinosaur relationships and early dinosaur evolution. *Nature* **543**, 501–506 (2017).
14. J. A. Gauthier, Saurischian monophyly and the origin of birds. *Mem. California Acad. Sci.* **8**, 1–55 (1986).
15. K. F. Hirsch, B. Quinn, Eggs and eggshell fragments from the Upper Cretaceous Two Medicine Formation of Montana. *J. Vertebr. Paleontol.* **10**, 491–511 (1990).
16. D. J. J. van Hinsbergen, L. V. de Groot, S. J. van Schaik, W. Spakman, P. K. Bijl, A. Sluijs, C. G. Langereis, H. Brinkhuis, A paleolatitude calculator for paleoclimate studies. *PLOS ONE* **10**, e0126946 (2015).
17. R. A. Spicer, A. B. Herman, The late Cretaceous environment of the Arctic: A quantitative reassessment based on plant fossils. *Palaeogeogr. Palaeoclimatol. Palaeoecol.* **295**, 423–442 (2010).
18. R. Amiot, C. Lécuyer, E. Buffetaut, F. Fluteauc, S. Legendre, F. Martineau, Latitudinal temperature gradient during the cretaceous upper campanian–middle maastrichtian: $\delta^{18}O$ record of continental vertebrates. *Earth Planet. Sci. Lett.* **226**, 255–272 (2004).
19. C. G. Panaiotu, C. E. Panaiotu, Palaeomagnetism of the upper cretaceous sânpetru formation (Haţeg Basin, South Carpathians). *Palaeogeogr. Palaeoclimatol. Palaeoecol.* **293**, 343–352 (2010).
20. S. J. Hunter, P. J. Valdes, A. M. Haywood, P. J. Markwick, Modelling Maastrichtian climate: investigating the role of geography, atmospheric $CO_2$ and vegetation. *Clim. Past Discuss.* **4**, 981–1019 (2008).
21. G. R. Upchurch, J. Kiehl, C. Shields, J. Scherer, C. Scotese, Latitudinal temperature gradients and high-latitude temperatures during the latest Cretaceous: Congruence of geologic data and climate models. *Geology* **43**, 683–686 (2015).
22. R. Prinzinger, A. Preβmar, E. Schleucher, Body temperature in birds. *Comp. Biochem. Physiol.* **99**, 499–506 (1991).
23. F. Seebacher, R. M. Elsey, P. L. Trosclair III, Body temperature null distributions in reptiles with nonzero heat capacity: seasonal thermoregulation in the American Alligator (*Alligator mississippiensis*). *Physiol. Biochem. Zool.* **76**, 348–359 (2003).
24. Southern Regional Climate Center, Rockefeller Wildlife Refuge Station Information, (Louisiana State University, Baton Rouge, LA, 2017); https://www.srcc.lsu.edu/.
25. A. E. McKechnie, B. G. Lovegrove, Avian facultative hypothermic responses: A review. *Condor* **104**, 705–724 (2002).
26. M. Daëron, D. Blamart, M. Peral, H. P. Affek, Absolute isotopic abundance ratios and the accuracy of $\Delta_{47}$ measurements. *Chem. Geol.* **422**, 83–96 (2016).
27. P. Ghosh, J. Adkins, H. Affek, B. Balta, W. Guo, E. A. Schauble, D. Schrag, J. M. Eiler, $^{13}C$–$^{18}O$ bonds in carbonate minerals: A new kind of paleothermometer. *Geochim. Cosmochim. Acta* **70**, 1439–1456 (2006).
28. S. Montanari, Cracking the egg: the use of modern and fossil eggs for ecological, environmental and biological interpretation. *R. Soc. Open Sci.* **5**, 180006 (2018).
29. K. E. Mikhailov, Palaeontological Association., *Fossil and Recent Eggshell in Amniotic Vertebrates: Fine Structure, Comparative Morphology and Classification*, Special papers in palaeontology, (Palaeontological Association, London, 1997).
30. D. K. Zelenitsky, L. V. Hills, An egg clutch of *Prismatoolithus levisoosp*. nov. from the Oldman Formation (Upper Cretaceous), Devil's Coulee, southern Alberta. *J. Can. Earth Sci.* **33**, 1127–1131 (1996).
31. D. J. Varricchio, J. R. Horner, F. D. Jackson, Embryos and eggs for the Cretaceous theropod dinosaur *Troodon formosus*. *J. Vertebr. Paleontol.* **22**, 564–576 (2002).
32. D. K. Zelenitsky, S. P. Modesto, P. J. Currie, Bird-like characteristics of troodontid theropod eggshell. *Cretac. Res.* **23**, 297–305 (2002).
33. D. K. Zelenitsky, L. V. Hills, Normal and pathological eggshells of *Spheroolithus albertensis*, oosp. nov., from the Oldman formation (Judith river group, late Campanian), southern Alberta. *J. Vertebr. Paleontol.* **17**, 167–171 (2010).
34. J. Van Itterbeeck, E. Sasaran, V. Codrea, L. Sasaran, P. Bultynck, Sedimentology of the Upper Cretaceous mammal- and dinosaur-bearing sites along the Râul Mare and Barbat rivers, Haeg Basin, Romania. *Cretac. Res.* **25**, 517–530 (2004).
35. G. Grellet-Tinner, V. Codrea, A. Folie, A. Higa, T. Smith, First evidence of reproductive adaptation to "island effect" of a dwarf Cretaceous Romanian Titanosaur, with embryonic integument in ovo. *PLOS ONE* **7**, e32051 (2012).

36. Z. Csiki, V. Codrea, C. Jipa-Murzea, P. Godefroit, A partial titanosaur (Sauropoda, Dinosauria) skeleton from the Maastrichtian of Nălaţ-Vad, Haţeg Basin, Romania. *Neues Jahrbuch Fur Geologie Und Palaontologie-Abhandlungen* **258**, 297–324 (2010).

37. K. Stein, Z. Csiki, K. C. Rogers, D. B. Weishampel, R. Redelstorff, J. L. Carballido, P. M. Sander, Small body size and extreme cortical bone remodeling indicate phyletic dwarfism in Magyarosaurus dacus (Sauropoda: Titanosauria). *Proc. Natl. Acad. Sci.* **107**, 9258–9263 (2010).

38. J. Le Loeuff, Romanian late cretaceous dinosaurs: big dwarfs or small giants? *Hist. Biol.* **17**, 15–17 (2005).

39. D. Grigorescu, The "Tuştea puzzle" revisited: Late Cretaceous (Maastrichtian) Megaloolithuseggs associated withTelmatosaurushatchlings in the Haţeg Basin. *Hist. Biol.* **29**, 627–640 (2016).

40. G. Botfalvai, Z. Csiki-Sava, D. Grigorescu, Ş. Vasile, Taphonomical and palaeoecological investigation of the Late Cretaceous (Maastrichtian) Tuştea vertebrate assemblage (Romania; Haţeg Basin) – insights into a unique dinosaur nesting locality. *Palaeogeogr. Palaeoclimatol. Palaeoecol.* **468**, 228–262 (2017).

41. M. J. Benton, Z. Csiki, D. Grigorescu, R. Redelstorff, P. M. Sander, K. Stein, D. B. Weishampel, Dinosaurs and the island rule: The dwarfed dinosaurs from Haţeg Island. *Palaeogeogr. Palaeoclimatol. Palaeoecol.* **293**, 438–454 (2010).

42. E. A. A. Versteegh, H. B. Vonhof, S. R. Troelstra, R. J. G. Kaandorp, D. Kroon, Seasonally resolved growth of freshwater bivalves determined by oxygen and carbon isotope shell chemistry. *Geochem. Geophys. Geosyst.* **11**, Q08022 (2010).

43. B. M. McAllan, F. Geiser, Torpor during reproduction in mammals and birds: dealing with an energetic conundrum. *Integr. Comp. Biol.* **54**, 516–532 (2014).

44. T. D. J. England, The University of British Columbia, Vancouver, Canada (1984).

45. A. Stilla, Géologie de la région de Haţeg-Cioclovina-Pui-Băniţa (Carpathes Méridionales). *Anuarul Institutului de Geologie şi Geofizica* **66**, 91–173 (1985).

46. J. G. Sclater, C. Jaupart, D. Galson, The heat flow through oceanic and continental crust and the heat loss of the Earth. *Rev. Geophys.* **18**, 269–311 (1980).

47. F. V. Paladino, M. P. O'Connor, J. R. Spotila, Metabolism of leatherback turtles, gigantothermy, and thermoregulation of dinosaurs. *Nature* **344**, 858–860 (1990).

48. J. R. Super, K. Chin, M. Pagani, H. Li, C. Tabor, D. M. Harwood, P. M. Hull, Late Cretaceous climate in the Canadian Arctic: Multi-proxy constraints from Devon Island. *Palaeogeogr. Palaeoclimatol. Palaeoecol.* **504**, 1–22 (2018).

49. G. M. Erickson, O. W. M. Rauhut, Z. H. Zhou, A. H. Turner, B. D. Inouye, D. Y. Hu, M. A. Norell, Was dinosaurian physiology inherited by birds? reconciling slow growth in Archaeopteryx. *PLOS ONE* **4**, e7390 (2009).

50. K. Schmidt-Nielsen, *Scaling: Why is Animal Size so Important?* (Cambridge Univ. Press., New York, NY, 1984).

51. M. S. Y. Lee, A. Cau, D. Naish, G. J. Dyke, Sustained miniaturization and anatomical innovation in the dinosaurian ancestors of birds. *Science* **345**, 562–566 (2014).

52. S. L. Brusatte, G. T. Lloyd, S. C. Wang, M. A. Norell, Gradual assembly of avian body plan culminated in rapid rates of evolution across the dinosaur-bird transition. *Curr. Biol.* **24**, 2386–2392 (2014).

53. P.-J. Chen, Z.-m. Dong, S.-n. Zhen, An exceptionally well-preserved Theropod dinosaur from the Yixian Formation of China. *Nature* **391**, 147–152 (1998).

54. P. S. Godefroit, M. Sofia, D. Dhouailly, Y. L. Bolotsk, A. V. Sizov, M. E. McNamara, M. J. Benton, P. Spagna, A Jurassic ornithischian dinosaur from Siberia with both feathers and scales. *Science* **345**, 451–455 (2014).

55. Z. Yang, B. Jiang, M. E. McNamara, S. L. Kearns, M. Pittman, T. G. Kaye, P. J. Orr, X. Xu, M. J. Benton, Pterosaur integumentary structures with complex feather-like branching. *Nat. Ecol. Evol.* **3**, 24–30 (2019).

56. P. M. J. Douglas, H. P. Affek, L. C. Ivany, A. J. P. Houben, W. P. Sijp, A. Sluijs, S. Schouten, M. Pagani, Pronounced zonal heterogeneity in Eocene southern high-latitude sea surface temperatures. *Proc. Natl. Acad. Sci. U.S.A.* **111**, 6582–6587 (2014).

57. R. E. Came, U. Brand, H. P. Affek, Clumped isotope signatures in modern brachiopod carbonate. *Chem. Geol.* **377**, 20–30 (2014).

58. S. Zaarur, H. P. Affek, M. Stein, Last glacial-Holocene temperatures and hydrology of the Sea of Galilee and Hula Valley from clumped isotopes in Melanopsis shells. *Geochim. Cosmochim. Acta* **179**, 142–155 (2016).

59. D. Evans, N. Sagoo, W. Renema, L. J. Cotton, W. Muller, J. A. Todd, P. K. Saraswati, P. Stassen, M. Ziegler, P. N. Pearson, P. J. Valdes, H. P. Affek, Eocene greenhouse climate revealed by coupled clumped isotope-Mg/Ca thermometry. *Proc. Natl. Acad. Sci. U.S.A.* **115**, 1174–1179 (2018).

60. J. Werner, E. M. Griebeler, New insights into non-avian dinosaur reproduction and their evolutionary and ecological implications: linking fossil evidence to allometries of extant close relatives. *PLOS ONE* **8**, e72862 (2013).

61. D. A. Eberth, D. B. Brinkman, Paleoecology of an estuarine, incised-valley fill in the Dinosaur Park Formation (Judith River Group, Upper Cretaceous) of Southern Alberta, Canada. *Palaios* **12**, 43–58 (1997).

62. D. A. Eberth, A. P. Hamblin, Tectonic, stratigraphic, and sedimentologic significance of a regional discontinuity in the Upper Judith River Group (Belly River Wedge) of Southern Alberta, Saskatchewan, and Northern Montana. *Can. J. Earth Sci.* **30**, 174–200 (1993).

63. F. Therrien, D. K. Zelenitsky, K. Tanaka, W. J. Sloboda, in *Hadrosaurs*, D. A. Eberth, D. C. Evans, Eds. (Indiana Univ. Press, Bloomington, 2014), pp. 532–539.

64. J. R. Horner, P. J. Currie, in *Dinosaur Eggs and Babies*, K. F. H. Ken Carpenter, John R. Horner, Ed. (Cambridge Univ. Press, 1994), chap. 21, pp. 312–336.

65. G. A. Henkes, B. H. Passey, E. L. Grossman, B. J. Shenton, A. Perez-Huerta, T. E. Yancey, Temperature limits for preservation of primary calcite clumped isotope paleotemperatures. *Geochim. Cosmochim. Acta* **139**, 362–382 (2014).

66. F. Therrien, Palaeoenvironments of the latest Cretaceous (Maastrichtian) dinosaurs of Romania: Insights from fluvial deposits and paleosols of the Transylvanian and Haţeg basins. *Palaeogeogr. Palaeoclimatol. Palaeoecol.* **218**, 15–56 (2005).

67. C. T. Rueden, J. Schindelin, M. C. Hiner, B. E. Dezonia, A. E. Walter, E. T. Arena, K. W. Eliceiri, ImageJ2: ImageJ for the next generation of scientific image data. *BMC Bioinformatics* **18**, 529 (2017).

68. J. Schindelin, I. Arganda-Carreras, E. Frise, V. Kaynig, M. Longair, T. Pietzsch, S. Preibisch, C. Rueden, S. Saalfeld, B. Schmid, J.-Y. Tinevez, D. J. White, V. Hartenstein, K. Eliceiri, P. Tomancak, A. Cardona, Fiji, An open-source platform for biological-image analysis. *Nat. Methods* **9**, 676–682 (2012).

69. H. P. Affek, J. M. Eiler, Abundance of mass 47 $CO_2$ in urban air, car exhaust, and human breath. *Geochim. Cosmochim. Acta* **70**, 1–12 (2006).

70. K. W. Huntington, J. M. Eiler, H. P. Affek, W. Guo, M. Bonifacie, L. Y. Yeung, N. Thiagarajan, B. Passey, A. Tripati, M. Daëron, R. Came, Methods and limitations of 'clumped' $CO_2$ isotope ($\Delta_{47}$) analysis by gas-source isotope ratio mass spectrometry. *J. Mass Spectrom.* **44**, 1318–1329 (2009).

71. K. J. Dennis, H. P. Affek, B. H. Passey, D. P. Schrag, J. M. Eiler, Defining an absolute reference frame for 'clumped' isotope studies of $CO_2$. *Geochim. Cosmochim. Acta* **75**, 7117–7131 (2011).

72. Ø. Hammer, D. A. T. Harper, P. D. Ryan, PAST:Paleontological Statistics software package for education and data analysis. *Palaeontol. Electron.* **4**, 9 (2001).

73. T. Kluge, H. P. Affek, Quantifying kinetic fractionation in Bunker Cave speleothems using $\Delta_{47}$. *Quat. Sci. Rev.* **49**, 82–94 (2012).

74. S.-T. Kim, A. Mucci, B. E. Taylor, Phosphoric acid fractionation factors for calcite and aragonite between 25 and 75 °C: Revisited. *Chem. Geol.* **246**, 135–146 (2007).

75. J. R. Kelson, K. W. Huntington, A. J. Schauer, C. Saenger, A. R. Lechler, Toward a universal carbonate clumped isotope calibration: Diverse synthesis and preparatory methods suggest a single temperature relationship. *Geochim. Cosmochim. Acta* **197**, 104–131 (2017).

# Science Advances

Robin R. Dawson, Daniel J. Field, Pincelli M. Hull, Darla K. Zelenitsky, François Therrien and Hagit P. Affek

| | |
|---|---|
| **ARTICLE TOOLS** | http://advances.sciencemag.org/content/6/7/eaax9361 |
| **SUPPLEMENTARY MATERIALS** | http://advances.sciencemag.org/content/suppl/2020/02/10/6.7.eaax9361.DC1 |
| **REFERENCES** | This article cites 68 articles, 11 of which you can access for free http://advances.sciencemag.org/content/6/7/eaax9361#BIBL |
| **PERMISSIONS** | http://www.sciencemag.org/help/reprints-and-permissions |

Use of this article is subject to the Terms of Service